Journal of Aerosol Science 105 (2017) 84–93

Contents lists available at ScienceDirect

Journal of Aerosol Science

journal homepage: www.elsevier.com/locate/jaerosci

Thermophoresis deposition studies for NaCl and diesel exhaust particulate matter under laminar flow

S.S. Bhusnoor[a], U.V. Bhandarkar[b], V. Sethi[c,*], P.P. Parikh[b]

[a] Department of Mechanical Engineering, K.J.Somaiya College of Engineering, Vidyavihar, Mumbai-400077, India
[b] Department of Mechanical Engineering, Indian Institute of Technology Bombay, Mumbai-400076, India
[c] Centre for Environmental Science and Engineering, Indian Institute of Technology Bombay, Mumbai-400076, India

ARTICLE INFO

Keywords:
Thermophoretic deposition
Axially decreasing wall temperature
Engine exhaust
Laminar flow
Particle thermal conductivity

ABSTRACT

Deposition of fine particles is acknowledged as a concern in various processes. Previous studies have investigated thermophoretic transport for various flow regimes (~30 < Re < 1400), particle sizes (0.01 to 8 μm), and temperature ranges of 25 to 145 °C and 425 to 580 °C. An experimental setup was developed to study thermophoretic deposition for particles near ~1 μm size, in the 170 < T_{gas} < 360 °C temperature range, similar to the conditions of exhaust from the diesel engine used in the present study. NaCl test aerosols (Mass mean diameter (MMD) 0.32 and 0.61 μm), and diesel exhaust particles (MMD 0.44, 0.35 and 0.29 μm) were used at gas inlet temperatures of 170, 260 and 360 °C, and 400 < Re < 2000. A model was developed to predict thermophoretic deposition under laminar flow in a pipe with an axially decreasing wall temperature. Use of a thermal conductivity (k_p) value of 0.5 W m^{-1} K^{-1} for engine exhaust particles in the model, was found to best match with the experimental observations. For both kinds of particles, the model developed in the present work performed as well as other existing models in the literature.

1. Introduction

Control of engine exhaust particle emissions remains an important research area for reasons of health (Donaldson, Stone, Gilmour, Brown, & MacNee, 2000; Kagawa, 2002) and environment (Lloyd & Cackette, 2001). This has been addressed by development of better engines and treatment of exhaust gases (Suzuki, Kuwana, & Dobashi, 2009; Strom & Sasic, 2012). There is a need to better understand the transport behaviour of diesel engine exhaust particulate matter (PM) for design towards more efficient control approaches. Besides this, deposition of fine particles is acknowledged as a concern in various processes such as fouling in heat exchangers, contamination in microelectronics, sample collection of atmospheric particles, losses in nanopowder production and deposition in turbines. Most such gas streams have particles in the sub-micrometer size range, which are subject several transport mechanisms including diffusion, turbulent impaction, thermophoresis, and electrophoresis. Particle laden gas streams that are at a temperature higher than the downstream equipment have the potential of utilising thermophoresis for particle removal. Such an understanding could also be utilised for prevention of deposition in situations such as sampling, fouling and contamination. Efforts towards development of a thermophoretic precipitator have been reported by Messerer, Niessner and Poschl (2004), Chien, Huang and Tsai (2009).

Several studies reported in literature have addressed theoretical and experimental aspects of thermophoretic (TP) deposition

* Corresponding author.
E-mail address: vsethi.iitb@gmail.com (V. Sethi).

http://dx.doi.org/10.1016/j.jaerosci.2016.11.011
Received 13 December 2015; Received in revised form 8 November 2016; Accepted 25 November 2016
Available online 07 December 2016
0021-8502/

Nomenclature

A_i	Pipe inside area (m^2)
A_o	Pipe outside area (m^2)
C_m	Momentum exchange coefficient = 1.14
C_p	Specific heat of the gas (kJ kg^{-1} K^{-1})
C_s	Thermal slip coefficient = 1.17
C_t	Temperature jump coefficient = 2.18
C_u	Slip correction factor
d_p	Particle diameter (μm)
d_t	Pipe diameter (m)
dA	Elementalarea = $\pi d_t dx$ (m^2)
dn	Change in concentration (g m^{-3})
dx	Elemental length (m)
FEG-SEM	Field Emission Gun - Scanning Electron Microscopy
h_i	Convective heat transfer coefficient of gas on the pipe inner surface (W m^{-2} K^{-1})
h_o	Convective heat transfer coefficient of air on the pipe outer surface (W m^{-2} K^{-1})
$\bar{h}$	Average convective heat transfer coefficient (W m^{-2} K^{-1})
k_g	Thermal conductivity of gas (W m^{-1} K^{-1})
k_p	Thermal conductivity of particle (W m^{-1} K^{-1})
k_t	Thermal conductivity of pipe (W m^{-1} K^{-1})
K_{th}	Thermophoretic coefficient
Kn	Knudsen number
L	Pipe length (m)
MMD	Mass Mean Diameter (μm)
MOUD	Micro Orifice Uniform Deposition Impactor
$\dot{m}$	Mass flow rate (kg s^{-1})
n	Particle concentration (g m^{-3})
n_i	Particle concentration at inlet (g m^{-3})
n_o	Particle concentration at outlet (g m^{-3})
Nu	Nusselt number
p	Perimeter of the pipe (m)
PM	Particulate Matter
Pr	Prandtl number
PSD	Particle Size Distribution
Q	Volumetric flow rate (m^3 s^{-1})
r_i	Pipe inner radius (m)
r_o	Pipe outer radius (m)
Re	Reynolds number
SSI	Single Stage Impactor
T_a	Ambient temperature (°C)
T_{ag}	Mean film temperature (°C)
T_{gas}	Exhaust gas temperature (°C)
$T_{m(i)}$	Gas mean temperature inlet to the pipe (°C)
$T_{m(o)}$	Gas mean temperature outlet of the pipe (°C)
$T_{m(x)}$	Gas mean temperature at axial position x (°C)
$T_{w(x)}$	Pipe wall temperature at axial psotion x (°C)
TP	Thermophoretic
V_{th}	Thermophoretic velocity (m s^{-1})
x	Distance from the entrance (m)

Greek Symbols

$(\nabla T) = dT/dr$	Radial temperature gradient (K m^{-1})
Δx	Elemental length (m)
η_{th}	Thermophoretic deposition efficiency
λ	Mean free path
μ_g	Dynamic viscosity of the gas (N s m^{-2})
μ_w	Dynamic viscosity of the fluid near the wall (N s m^{-2})
ρ_g	Density of the gas (kg m^{-3})

(Montassier, Boulaud, & Renoux, 1991; Stratmann, Otto, & Fissan, 1994; Tsai, Lin, Aggarwal, & Chen, 2004). Assessment of relative dominance of various transport mechanisms, such as thermophoresis and diffusion, under laminar and turbulent flow conditions, is the first step while considering such studies for a specific application. Thermophoresis is more dominant than diffusion in the 0.01–1 μm size ranges by 1 to 3 orders of magnitude under laminar flow (He & Ahmadi, 1998; Walker, Homsy, & Geyling, 1979; Tsai & Lu, 2004; Messerer, Niessner, & Poschl, 2004).

Previous studies have investigated thermophoretic transport for various flow regimes (~30 < Re < 1400) (Stratmann, Otto, & Fissan, 1994; Tsai, Lin, Aggarwal, & Chen, 2004; Munoz-Bueno, Hontañón, & Rucandio, 2005) and particle sizes (0.01–8 μm) (Montassier, Boulaud, & Renoux, 1991; Tsai, Lin, Aggarwal, & Chen, 2004; Munoz-Bueno, Hontañón, & Rucandio, 2005). The temperature ranges of these studies broadly fall into two ranges, namely ~25–145 °C (Stratmann, Otto, & Fissan, 1994; Romay, Takagaki, Pui, & Liu, 1998), and 425–580 °C (Munoz-Bueno, Hontañón, & Rucandio, 2005). Studies in the 150–450 °C temperature range, which is the typical range for engine exhaust (Hwang, Han, Yun, Kim, & Kim, 2005; Lee, Byun, Bae, & Lee, 2006; Messerer, Niessner, & Poschl, 2003), are limited. Further, the approach of most of the previous studies has been to use a constant wall temperature for the entire length of the pipe. In actual processes, such as soot laden flow in an engine exhaust, this constraint would need to be relaxed.

The focus of the present study was twofold. First, to develop a model for thermophoretic deposition in laminar flow in a pipe with an axially decreasing wall temperature condition based on reported literature; and second, to develop an experimental setup to study thermophoretic deposition for particles with dp < 1.0 μm size, in the 170 < T_{gas} < 360 °C temperature range, as conditions of particle size and temperatures in an engine exhaust respectively.

2. Materials and methods

The design of the experimental setup was intended such that it could be utilised to study thermophoretic deposition of particles with different properties and different sources. Further, it was also intended to fulfil on the requirements of experimental validation of the model simulations for thermophoretic deposition with reasonable accuracy. The focus was to first use the well studied NaCl test aerosols, followed by diesel particulate matter from an engine with sizes and concentrations matched by the test aerosols.

The bench scale particle deposition setup was developed with a pipe for laminar flow (400 < Re < 2000) with two kinds of

particulate matter: (1) Test aerosols generated using an NaCl solution in an atomiser, and (2) exhaust particulate matter from a stationary diesel engine. The setup was made of three main components (Fig.1): (a) an NaCl test aerosol generation and conditioning system; (b) a diesel engine with exhaust particle conditioning system; and (c) a pipe of 1 m length made up of 10 equal sections for deposition of particles by thermophoresis. The pipe sections were designed to have flushed smooth joints internally when assembled.

Subsystems (a) and (c) (Fig. 1), constituted the bench scale experimental setup for thermophoretic deposition analysis of NaCl test aerosols. An atomizer (TSI 3079) was used to generate NaCl test aerosols at 40 g/l and 300 g/l solution concentrations, which were dried and diluted with heated air to obtain the required temperatures for the deposition studies. Table 1 lists the particle sizes and mass concentrations. Subsystems (b) and (c) (Fig. 1), constituted the engine experimental setup for engine exhaust particulate matter. A plenum was included in the engine exhaust setup to suppress the pulsatile nature of flow and provide 12–20 s of residence time. At the plenum exit, the gas stream was heated to the required temperature range using a heater. The test aerosol and the engine exhaust were selected to be within the same particle size and concentration ranges. Changes in particle size distributions by condensation and coagulation were considered to be negligible based on low number concentrations, sub-saturation conditions, and aging prior to introducing the aerosols in the test section.

Mass deposition was measured using three approaches: (1) for both NaCl and engine exhaust particles, by comparing the particle size distributions (PSD) at the inlet and outlet of the one-meter pipe using Micro Orifice Uniform Deposition Impactor (MOUDI, 10-stage cascade impactor, 0.056 to 18 μm) (Park, Cao, Kittelson, & McMurry, 2003; Grose, Sakurai, Savstrom, Stolzenburg, Watts, Morgan, & McMurry, 2006). The aerosol dynamics were considered to have been quenched by the 10–12 times dilution with clean dry air before sampling, and the impaction based size distribution measurements in MOUDI, averaged over time were considered to be adequate; (2) for NaCl, by eluting the deposited particles inside the test sections with distilled water, followed by measurement of electrical conductivity of the eluted solution as an indicator of the amount of particles deposited in each of the 10 cm section; and (3) for engine exhaust particles, samples were diluted by 10–12 times with clean dry air, and a single stage impactor (SSI) with a cut-off particle size of 1 μm was used. Experimental conditions for the present study are listed in Table 1.

3. Development of the model

The model in this study was developed using a one-dimensional control volume approach (Romay, Takagaki, Pui, & Liu, 1998), for the estimation of thermophoretic deposition for the conditions expected in the engine exhaust ($0.056 < d_p < 5.6$ μm and $170 < T_{gas} < 360$ °C), by incorporating natural convective cooling and the resultant axial decrease in the pipe wall temperature, and the effect of temperature on gas properties (Li & Davis, 1995). The model assumes that the particles are spherical, the concentration is uniform at each cross section, and the internal surface of the pipe is smooth. A differential fluid element was considered at any particular pipe cross section of area dA as shown in Fig. 2. The particle fluxes into and out of the element, as well as the loss due to thermophoretic deposition were evaluated, and followed by integration over the entire length of the pipe. The focus on laminar regime was deliberate. While under turbulent regime, other transport mechanisms are likely to be more dominant, thermophoresis is the most dominant under laminar conditions for particles in the said size and temperatures ranges of interest in the present study (He & Ahmadi, 1998; Walker, Homsy, & Geyling, 1979).

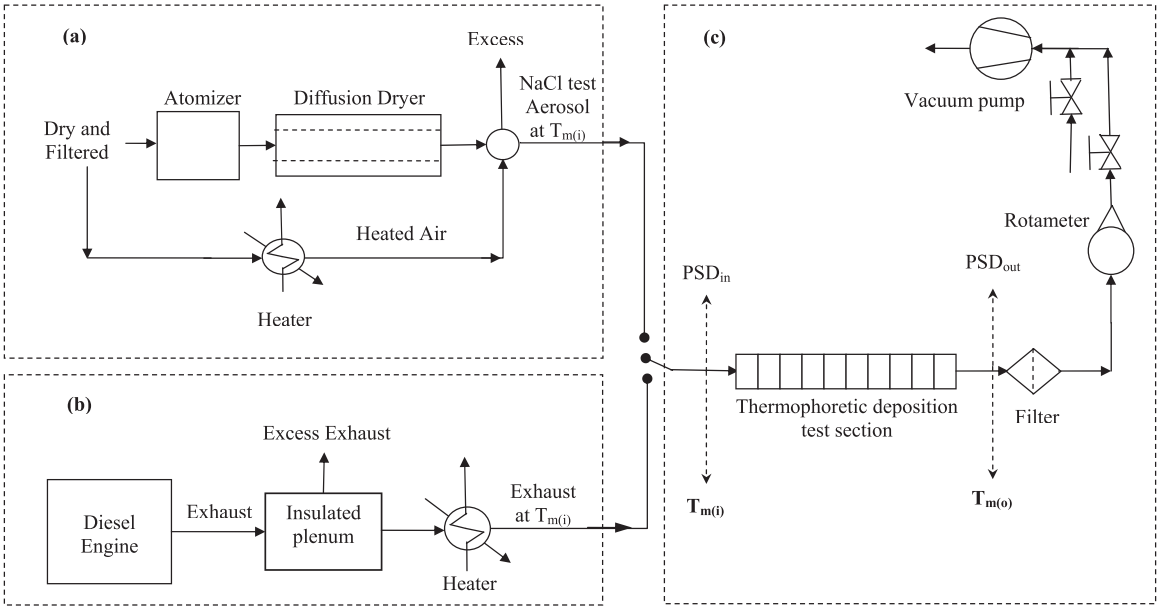

Fig. 1. Schematic diagram of experimental setup for study of thermophoretic deposition: Subsystems (a) and (c) constitute the bench scale setup for NaCl test aerosols; and (b) and (c) constitute the setup for engine exhaust particulate matter.

Table 1
Experimental conditions for bench scale studies for thermophoretic deposition of NaCl test aerosols and diesel engine exhaust particulate matter.

Parameter	NaCl Test Aerosol	Engine Exhaust Particulate Matter
Particle size (MMD), μm	0.32 and 0.61	0.44, 0.35 and 0.29
Geometric standard deviation	1.60	1.30–1.96
Mass Concentrations at inlet (kg/m^3)	5.20E-6, 1.95E-5	2.01E-5, 5.43E-6 & 3.48E-6
Inlet temperatures (°C)	170, 260 and 360	170, 260 and 360
Room air temperature (°C)	27–31	27–31
Re	500, 700, 1000, 1200, 1400, 1800 and 2000	400, 700, 1000, 1300, 1700 and 2000
Particle source	TSI 3079 Atomiser with NaCl solution	Single cylinder, 4-stroke, diesel engine (5HP, 1500 rpm), exhaust temperature at full load ~360 °C. Fuel used is High speed diesel fuel with 50 ppm sulphur
Conditions	40 g/l and 300 g/l NaCl Solution concentration	Idling, 50% of full load and 100% of full load
Dimensions of pipe test section (Material)	15 mm inner diameter, 3 mm thickness, 100 cm length (10 × 10 cm test sections) (Mild steel, k_t = 15.5 W/mK)	

For the given differential element Δx, pipe diameter d_t, the change in concentration between inlet and outlet of the element can be expressed as:

$$\frac{dn}{n} = \frac{-\pi d_t V_{th} dx}{Q}. \tag{1}$$

In this Eq. (1), Q is the flow rate (m^3 s^{-1}) and V_{th} is the thermophoretic velocity (m s^{-1}) of the particle in a gas subjected to a temperature gradient and is given by the following expression:

$$V_{th} = -\frac{\mu_g}{\rho_g}\frac{K_{th}}{T_{ag}}(\nabla T), \tag{2}$$

Here μ_g and ρ_g are the dynamic viscosity and density of the gas respectively, T_{ag} is the mean film temperature in the element, ∇T is the temperature gradient towards the wall (dT/dr in the present case) and K_{th} is the thermophoretic coefficient. Among the various expressions for the thermophoretic coefficient available in the literature, the generally accepted expression for a wide range of Knudsen number (Kn) given by Talbot, Cheng, Schefer, and Willis (1980) was used for the model in the present work, expressed as:

$$K_{th} = \frac{2C_s(k_g/k_p + C_t Kn)C_u}{(1 + 3C_m Kn)(1 + 2(k_g/k_p) + 2C_t Kn)}, \tag{3}$$

where, C_u, C_m, C_s and C_t are slip correction factor, momentum exchange coefficient, thermal slip coefficient and temperature jump coefficient respectively, and k_g and k_p are the thermal conductivities of the gas and particle respectively.

To derive the expression for temperature gradient, a pipe of length L and diameter d_t was considered (Fig. 2), with flow rate of gas Q (m^3 s^{-1}), inlet temperature $T_{m(i)}$ (°C), exit temperature $T_{m(o)}$ (°C), inlet concentration n_i (kg m^{-3}), and exit concentration n_o (kg m^{-3}). By equating conductive and convective heat transfer rates at the wall for the fluid element, the following expression is obtained:

$$k_g \left.\frac{dT(x)}{dr}\right|_{r=r_i} = \bar{h}\,[T_w(x) - T_m(x)], \tag{4}$$

where, $T_w(x)$ and $T_m(x)$ are the pipe surface temperature and the gas mean temperatures at any section along the pipe axis respectively, and $\bar{h}$ is the average convective heat transfer coefficient. Temperature variation from the centre of the pipe to the wall was assumed to be linear. The average convective heat transfer coefficient ($\bar{h}$) in Eq. (4) was calculated using the Nusselt number (Nu). When the difference between the surface and fluid temperature is large, it may be necessary to account for the variation of

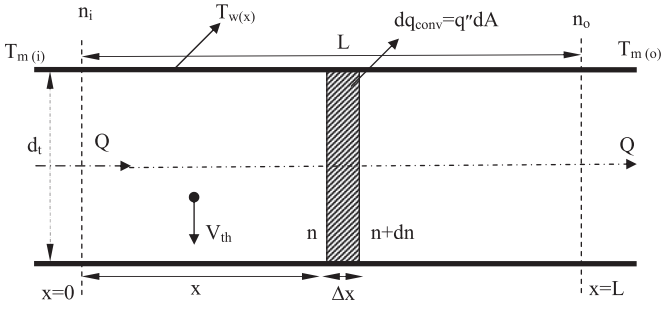

Fig. 2. Control element for analysis by thermophoretic deposition.

viscosity with temperature. For the present study, the following expression for average Nu by Sieder and Tate, for developing flow in a pipe was used (Incropera & DeWitt, 1996):

$$Nu = \frac{\bar{h} d_t}{k_g} = 1.86\left[\frac{\mathrm{Re}\,\mathrm{Pr} d_t}{L}\right]^{0.666}\left[\frac{\mu}{\mu_w}\right]^{0.14}, \tag{5}$$

where, Re is Reynolds number, Pr is Prandtl number, L is pipe length and μ_w is the dynamic viscosity of the fluid at the wall temperature. The axial decrease in the temperature of the gas can be evaluated by equating the axial drop in the gas enthalpy to the convective heat lost to the walls in the corresponding length. The resulting expression is as follows:

$$\frac{dT(x)}{dx} = \frac{p\bar{h}\,[T_w(x) - T_m(x)]}{\dot{m} C_p}. \tag{6}$$

Here, p is the perimeter of the pipe ($p = \pi d_t$), C_p (J kg^{-1} K^{-1}) is the specific heat of the gas and $\dot{m}$ (kg s^{-1}) is the mass flow rate of the gas. By applying steady flow energy equation for flow of heat from gas to wall and from the wall to the surroundings, the surface temperature along the pipe length can be expressed as:

$$T_w(x) = \frac{[(h_i A_i)(\ln(r_o/r_i)/(2\pi k_t L)) + ((h_i A_i)(1/(h_o A_o)))]T_m(x) + T_a}{[1 + (\ln(r_o/r_i)/(2\pi k_t L))(h_i A_i) + (h_i A_i)(1/(h_o A_o))]}. \tag{7}$$

Eqs. (6) and (7) are solved numerically to get the mean gas temperature and wall temperature along the length of the one-meter pipe test section setup. The suitability of this approach was justified by predicting the gas temperature at the exit of the pipe for all experimental conditions. Using this approach, the predictions of the exit temperatures were found to be within ± 4 °C of the experimental values for the gas temperatures. The wall temperatures were estimated based on the calculations of gas temperatures, and were considered acceptable since the gas temperatures matched well with the experiments. Sensitivity of wall temperature to conductivity of the pipe material was found to be insignificant.

Using the value of $T_{m(x)}$ and $T_{w(x)}$ at any given "x", the radial temperature gradient was found using Eq. (4), where $\dot{m}$ is found using Eq. (5). This gradient along with K_{th} (Eq. (3)) was then used to get V_{th} (Eq. (2)) at any "x". The deposition rate (Eq. (1)) was calculated and integrated from the inlet to a distance "x", yielding the following expression for the thermophoretic deposition efficiency:

$$\eta_{th} = 1 - \exp\left\{\frac{-\mathrm{Pr} K_{th} k_g (T_m(x) - T_w(x))\left[1 - \exp\left|-\frac{\pi d_t \bar{h} x}{\dot{m} C_p}\right|\right]}{k_g\left[\frac{T_m(x) + T_w(x)}{2}\right]}\right\}. \tag{8}$$

This expression was used to estimate the thermophoretic deposition for the inlet conditions listed in Table 1, discussed in the next section.

4. Results and discussion

The measured thermophoretic deposition efficiencies of NaCl test aerosols and diesel exhaust particulate matter ($0.03 < Kn < 5.05$, $0.056 < d_p < 5.6$ μm and $170 < T_{gas} < 360$ °C) were compared with model predictions. The effect of gas flow rate (Re), gas inlet temperatures and particle sizes on thermophoretic deposition are discussed in this section. The particle sizes as cut-off sizes in MOUDI for both NaCl and exhaust particles were validated using Field Emission Gun - Scanning Electron Microscope (*FEG-SEM)* image analysis for each stage of MOUDI (Fig. 3). Particle sizes were found to be in reasonable agreement.

The size distribution for one of the NaCl solution strengths, *viz.* 40 g/l (0.32 μm MMD, 1.60 GSD) in the aerosol generator is shown in Fig. 4, along with the three different size distribution measurements at the exit of the test pipe section corresponding to three different temperatures for Re = 500. Similar measurements were carried out for Re = 1000 and 1200 for 0.32 μm MMD, and further also for 0.61 μm MMD for Re values of 500, 1000 and 1200. The results of deposition as a function of size and Re for the case of 0.32 μm MMD NaCl test aerosol, are summarised in Fig. 5. Model predictions from Eq. (8) for the same conditions are also plotted in Fig. 5 for comparison. It was observed that in the particle size range of 0.056 to 0.32 μm, the experimental deposition efficiencies are independent of the size of the particle as expected (Hinds, 1999; Munoz-Bueno, Hontañón, & Rucandio, 2005; Santachiara, Prodia, & Cornettia, 2002). For particle sizes larger than 0.32 μm, there was a decrease in deposition rate as size of the particle increases. The trends were found to behave as per theoretical expectation.

Results for the effect of Re (500 to 2000) on the deposition are summarised in Fig. 6 along with the results of the model simulations for the respective conditions. As expected, the deposition for the smaller particle size (0.32 μm MMD) is higher than that for the larger particle size (0.61 μm MMD), higher for smaller Re, and higher for the higher gas inlet temperatures. Model results were found to underpredict the experimental observations, to within 14–17% for the entire range of the parametric space. A similar difference between experimental results and model predictions in the range of 3–24% has been reported in previous studies (Stratmann, Otto, & Fissan, 1994; Romay, Takagaki, Pui, & Liu, 1998; Tsai, Lin, Aggarwal & Chen, 2004).

For engine exhaust, the particle size distribution (PSD) measurements for the three temperatures (namely 170, 260 and 360 °C) are shown in Fig. 7, for Re 400. The PSD at the inlet of the deposition section were found to vary for the three temperatures. A similar

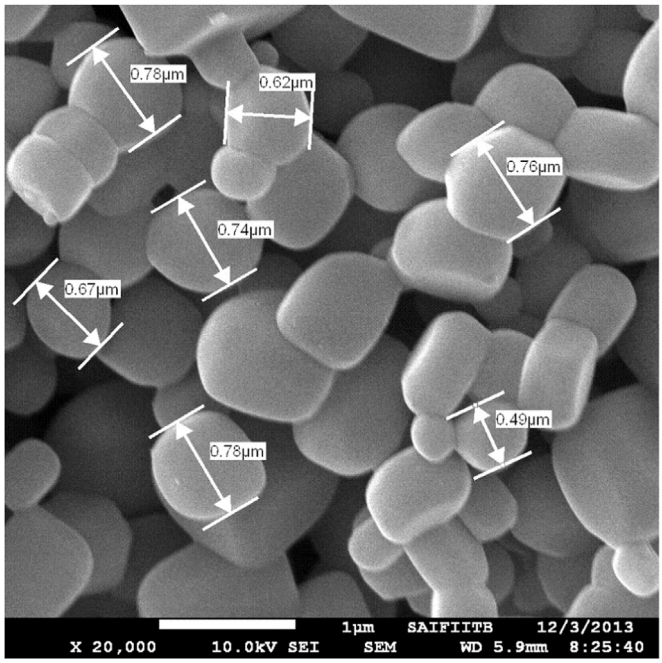

Fig. 3. FEG-SEM images of NaCl test aerosols collected on the sixth stage of MOUDI ($0.56 < d_p < 1$ µm).

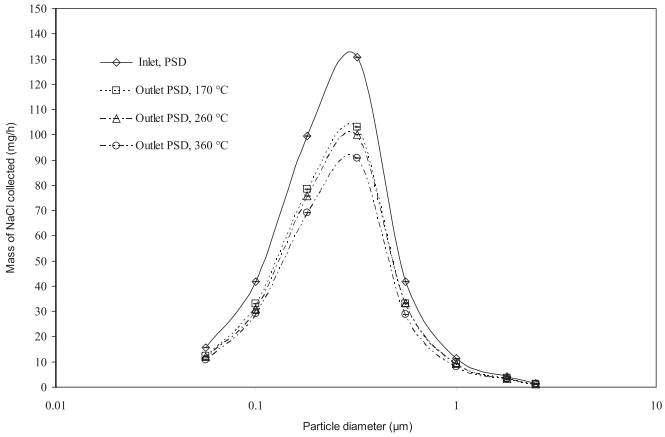

Fig. 4. Mass size distributions (PSD) of the NaCl test aerosols measured by using MOUDI at the inlet and the exit of the thermophoretic deposition test section at Re 500, and gas inlet temperatures of 170, 260 and 360 °C.

change in PSD due to change in inlet temperatures (30–360 °C) of the exhaust particles was also observed by Lee, Byun, Bae and Lee (2006), Messerer, Niessner and Poschl (2003).

The deposition efficiencies for the above conditions are plotted as Fig. 8, along with the model predictions. Fig. 8 shows that in the particle size range of 0.056–0.32 µm, the experimental deposition efficiencies are independent of the size of the particle as expected (Hinds, 1999; Munoz-Bueno, Hontañón, & Rucandio, 2005) and model results were found to underpredict the experimental observations. It also shows that there is decrease in thermophoretic deposition of particles of size greater than 0.32 µm MMD. This trend was also observed for NaCl as described earlier.

The results for deposition of engine exhaust particulate matter as a function of Re (400–2000) are summarised as Fig. 9 along with the model predictions. These deposition efficiencies are consistent with those obtained using sodium chloride test aerosols (Fig. 6). As in the case of NaCl particles, the model underpredicts the deposition of engine exhaust particulate matter between 10 and 18% (Fig. 9).

The influence of choice of particle thermal conductivity (k_p) was found to be critical in the study. Unlike the case of NaCl, where the value of k_p is well established, particulate matter from the engine exhaust are complex hydrocarbon particles and the value of k_p for such particles is not well known. Choosing either the conductivity of carbon as 4.2 W/mK (Hinds, 1999), or of soot particles in a fouling deposit layer as 0.041 W/mK (Lance, Sluder, Wang, & Storey, 2009), leads the model predictions to significantly deviate from the deposition rates observed in the present work (Fig. 10). A choice of $k_p = 0.5$ ($Wm^{-1} K^{-1}$) (Abarham, Hoard, Assanis, Styles,

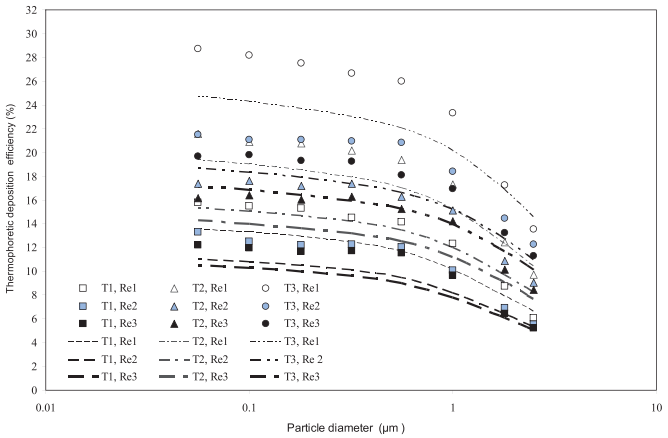

Fig. 5. Comparison of predicted thermophoretic deposition efficiency of NaCl test aerosols using present model as a function of particle size with experimental results obtained for sizes using MOUDI (Re1 = 500, Re2 = 1000, Re3 = 1200 and T1 = 170 ˚C, T2 = 260 ˚C, T3 = 360 ˚C) (Symbols represent experimental data and the various dashed lines represent the model predictions).

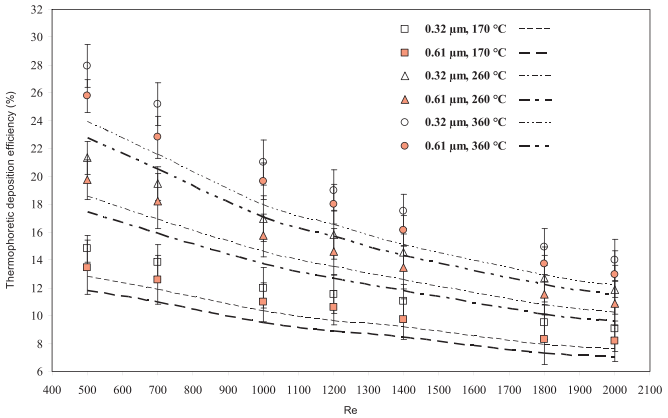

Fig. 6. Comparison of experimental thermophoretic deposition efficiency (for experimental matrix and conditions given in Table 1) of NaCl test aerosols with the predictions from the model developed in the present work. (Symbols represent experimental data and the various dashed lines represent the model predictions).

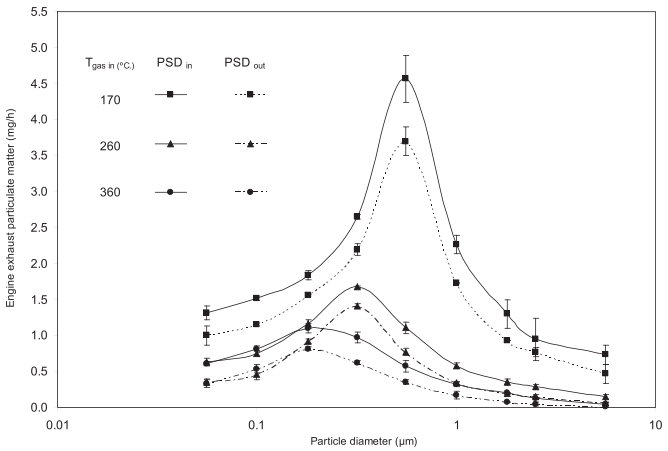

Fig. 7. Mass size distribution (PSD) of the engine exhaust particulate matter measured by using MOUDI at inlet and exit of the pipe at Re 400 and gas inlet temperatures of 170, 260 and 360 ˚C.

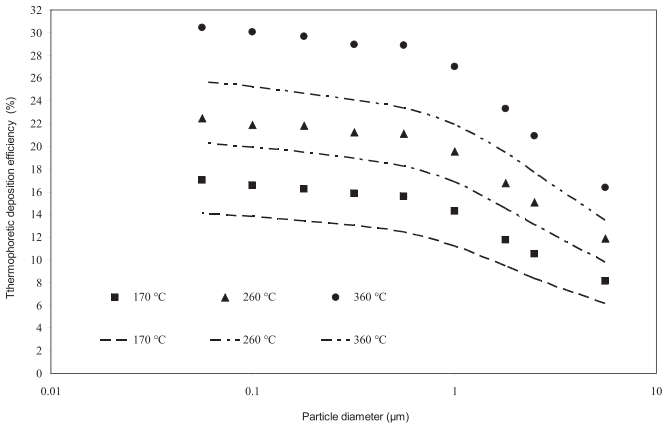

Fig. 8. Comparison of experimental deposition efficiencies of engine exhaust particles with model predictions at Re 400 as a function of particle size for gas inlet temperatures of 170, 260 and 360 °C. (Symbols represent experimental data and the various dashed lines represent the model predictions).

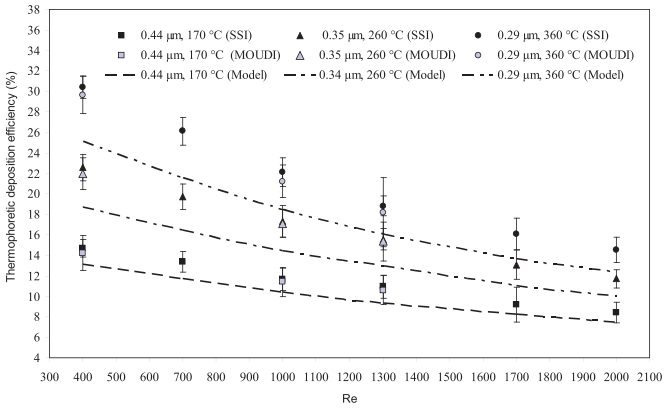

Fig. 9. Comparison of experimental thermophoretic deposition efficiency (for experimental matrix and conditions given in Table 1) of engine exhaust particulate matter using MOUDI and SSI, with the predictions from the model developed in the present work. (Symbols represent experimental data and the various dashed lines represent the model predictions).

Sluder, & Storey, 2010) instead, however, allowed for a good match between the model predictions and the experimental observations, and the same was applicable universally for all the inlet temperatures and the range of Re studied in the present work (Fig. 10). Further, Messerer, Niessner and Poschl (2003) have simulated diesel soot using graphite electrodes, and reported their experimental results to fit best with $k_p = 0.032\ W\ m^{-1}\ K^{-1}$. An equivalent comparison for NaCl which has a known value of thermal conductivity ($k_p = 6.6\ W\ m^{-1}\ K^{-1}$) is shown in Fig. 11.

5. Conclusions

Thermophoretic deposition of NaCl test aerosols and diesel engine exhaust particulate matter were studied ($0.03 < Kn < 5.05$, $0.056 < d_p < 5.6\ \mu m$ and $170 < T_{gas} < 360\ ^\circ C$) in a metal pipe under laminar flow, and the results were compared with those predicted by a model that was developed for this study. For both the model as well as the experiments, decrease in the wall temperature along the pipe length due to natural convection was incorporated, which is a significant difference in the present work. Model results were found to underpredict the experimental observations to within 14–17% for NaCl test aerosols and 10–18% for engine exhaust particulate matter for the range of the parametric space. This difference was seen to be comparable with the results reported in literature.

The experimental results in the present study showed that the thermophoretic coefficient expression given by Talbot et al. (1980), was applicable for exhaust particulate matter over a wide range of particle sizes and gas temperatures.

Morphology of particulate matter in diesel exhaust have been reported in previous studies, and further consideration of influence of these on thermophoretic transport may be important (Lee, Cole, Sekar, Choi, Kang, Bae & Shin, 2002; Park, Cao, Kittelson and McMurry, 2003; Virtanen, Ristimaki, Vaaraslahti & Keskinen, 2004). The choice of thermal conductivity (k_p) of particles, was relatively simple for NaCl, while for exhaust particles, a choice of 0.5 W/mK was found to be most suited as discussed earlier. Changes in particle size, structure and hydrocarbon content are highly dependent on the engine operating conditions and fuel quality. The use of an appropriate value of k_p for particles under different engine load conditions, as well as for particles encountered in other high temperature applications, such as fly ash in coal based power plants, cement industries, and metal industries, opens up questions for further investigations.

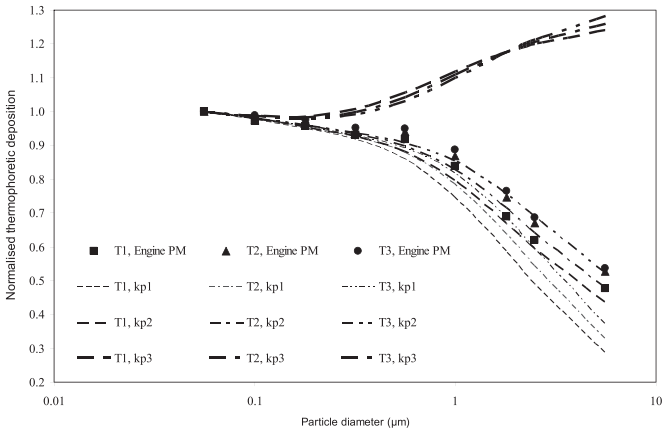

Fig. 10. Normalised thermophoretic deposition versus particle size for engine exhaust particulate matter at various gas inlet temperatures, Re 500, and predictions for a range of k_p values of carbon/soot from literature. k_p1, k_p2 and k_p3 are 4.2, 0.5 and 0.041 W/mK respectively. T1 = 170 °C, T2 = 260 °C, T3 = 360 °C. (Symbols represent experimental data and the various dashed lines represent the model predictions).

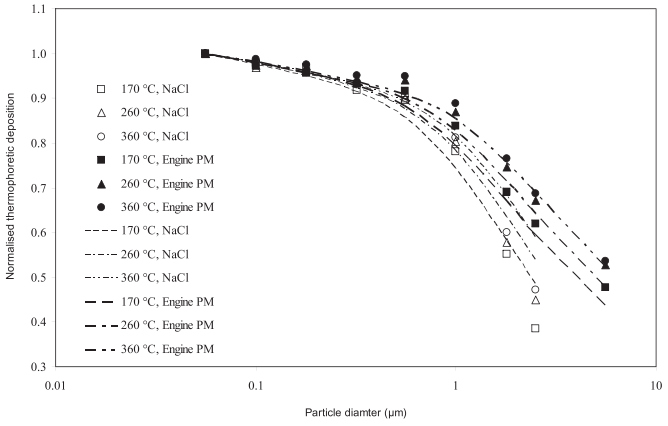

Fig. 11. Normalised thermophoretic deposition versus particle size at Re 500 and Re 400 for NaCl test aerosol and engine exhaust particulate matter respectively, at various gas inlet temperatures. (Symbols represent experimental data and the various dashed lines represent the model predictions).

Acknowledgements

We would like to thank Somaiya Trust Vidyavihar, Mumbai, India and Principal of K. J. Somaiya College of Engineering (KJSCE) for financial support for the development of bench scale setup at KJSCE. The first author would like to thank the staff of the Internal Combustion Engine Laboratory and the workshop of KJSCE for their support.

References

Abarham, M., Hoard, J. W., Assanis, D., Styles, D., Sluder, C. S., & Storey, J. M. E. (2010). An analytical study of thermophoretic particulate deposition in turbulent pipe flows. *Aerosol Science and Technology*, *44*, 785–795.

Chien, C. L., Huang, S. H., & Tsai, C. J. (2009). A new cross-flow tube bundle heat exchanger with staggered hot and cold tubes for thermophoretic deposition of submicron aerosol particles. *Aerosol Science and Technology*, 43, 1153–1163.

Donaldson, K., Stone, V., Gilmour, P., S., Brown, D. M., & MacNee, W. (2000). Ultrafine particles: mechanisms of lung injury. *Philosophical Transactions, the Royal Society*, *358*, 2741–2749.

Grose, M., Sakurai, M., Savstrom, J., Stolzenburg, M. R., Watts, J. R., Morgan, C. G., & McMurry Peter, H. (2006). Chemical and Physical Properties of Ultrafine Diesel Exhaust Particles Sampled Downstream of a Catalytic Trap. *Environmental Science and Technology*, *40*, *5502–5507*.

He, C., & Ahmadi, G. (1998). Particle deposition with thermophoresis in laminar and turbulent duct flows. *Aerosol Science and Technology*, *29*, 525–546.

Hinds, W. C. (1999). *Aerosol technology, properties, behavior, and measurement of air born particles* (2nd ed) New York: Wiley.

Hwang, S., Han, B., Yun, S., Kim, D., & Kim, Y. (2005). A study on the characteristics of exhaust particles from diesel engines with fuel injection types and after-treatment systems. *Particle and Aerosol Research*, *1*, 61–68.

Incropera, F. P., & DeWitt, D. P. (1996). *Fundamentals of heat and mass transfer* (3rd ed) New York: Wiley.

Kagawa, J. (2002). Health effects of diesel exhaust emissions - A mixture of air pollutants of worldwide concern. *Toxicology*, *181–182*, 349–353.

Lance, M. J., Sluder, C. S., Wang, H., & Storey, J. M. E. (2009). Direct measurement of EGR cooler deposit thermal properties for improved understanding of cooler fouling. *SAE International*, 2009–01-1461.

Lee, B. U., Byun, D. S., Bae, G., & Lee, J. (2006). Thermophoretic deposition of ultrafine particles in a turbulent pipe flow: Simulation of ultrafine particle behavior in an automobile exhaust pipe. *Journal of Aerosol Science*, *37*, 1788–1796.

Lee, K. O., Cole, R., Sekar, R., Choi, M. Y., Kang, J. S., Bae, C. S., & Shin, H. D. (2002). Morphologial investigation of microstructure, dimensions and fractal geometry of diesel particulates. *Proceedings of the Combustion Institute*, *29*, 647–653.
Li, W., & Davis, E. J. (1995). The effect of gas and particle properties on thermophoresis. *Journal of Aerosol Science*, *26*(*7*), 1085–1099.
Lloyd, A. C., & Cackette, T. A. (2001). Diesel engines: environmental impact and control. *Journal of the Air Waste Management Association*, *51*, *809*–847.
Messerer, A., Niessner, R., & Poschl, U. (2003). Thermophoretic deposition of soot aerosol particles under experimental conditions relevant for modern diesel engine exhaust gas systems. *Journal of Aerosol Science*, *34*, 1009–1021.
Messerer, A., Niessner, R., & Poschl, U. (2004). Miniature Pipe Bundle Heat Exchanger for Thermophoretic Deposition of Ultrafine Soot Aerosol Particles at High Flow Velocities. *Aerosol Science and Technology*, *38*, 456–466.
Montassier, N., Boulaud, D., & Renoux, A. (1991). Experimental study of thermophoretic particle deposition in laminar tube flow. *Journal of Aerosol Science*, *22*(5), 677–687.
Munoz-Bueno, R., Hontañón, E., & Rucandio, M. I. (2005). Deposition of fine aerosols in laminar tube flow at high temperature with large gas-to-wall temperature gradients. *Journal of Aerosol Science*, *36*, 495–520.
Park, K., Cao, F., Kittelson, D. B., & McMurry, P. H. (2003). Relationship between Particle Mass and Mobility for Diesel Exhaust Particles. *Environmental Science and Technology*, *37*, 577–583.
Romay, F. J., Takagaki, S. S., Pui, D. Y., & Liu, B. Y. (1998). Thermophoretic deposition of aerosol particles in turbulent pipe flow. *Journal of Aerosol Science*, *29*(8), 943–959.
Santachiara, G., Prodia, F., & Cornettia, C. (2002). Experimental measurements on thermophoresis in the transition region. *Journal of Aerosol Science*, *33*, 769–780.
Stratmann, F., Otto, E., & Fissan, H. (1994). Thermophoretical and diffusional particle transport in cooled laminar tube flow. *Journal of Aerosol science*, *25*(7), 1305–1319.
Strom, H., & Sasic, S. (2012). The role of thermophoresis in trapping of diesel and gasoline particulate matter. *Catalysis Today*, *188*, 14–23.
Suzuki, S., Kuwana, K., & Dobashi, R. (2009). Effect of particle morphology on thermophoretic velocity of aggregated soot particles. *International Journal of Heat and Mass Transfer*, *52*, 4695–4700.
Talbot, L., Cheng, R. K., Schefer, R. W., & Willis, D. R. (1980). Thermophoresis of particles in a heated boundary layer. *Journal of Fluid Mechanics*, *101*(4), 737–758.
Tsai, C. J., & Lu, H. (2004). Design and Evaluation of a Plate-to-Plate Thermophoretic Precipitator. *Aerosol Science and Technology*, *22*, 172–180.
Tsai, C. J., Lin, J. S., Aggarwal, S. G., & Chen, D-R. (2004). Thermophoretic deposition of particles in laminar and turbulent tube flows. *Aerosol Science and Technology*, *38*, 131–139.
Virtanen, A. K. K., Ristimaki, J. M., Vaaraslahti, K. M., & Keskinen, J. (2004). Effect of engine load on diesel soot particles. *Environmental Science and Technology*, *38*, 2551–2556.
Walker, K. L., Homsy, G. M., & Geyling, F. T. (1979). Thermophoretic deposition of small particles in laminar tube flow. *Journal of Colloid and Interface Science*, *69*(1), 138–147.